TÉCNICO LISBOA

Cooling System for Photovoltaic Panels

Maria Adelaide Nave Prata Cordeiro Ambrósio

Thesis to obtain the Master of Science Degree in

Electrical and Computer Engineering

Supervisor: Prof. João Paulo Neto Torres

Examination Committee

Chairperson: Prof. Célia Maria Santos Cardoso de Jesus
Supervisor: Prof. João Paulo Neto Torres
Member of the Committee: Prof. Paulo José da Costa Branco

February 2022

I declare that this document is an original work of my own authorship and that it fulfills all the requirements of the Code of Conduct and Good Practices of the Universidade de Lisboa.

Declaro que o presente documento e um trabalho original da minha autoria e que cumpre todos os requisitos do Codigo de Conduta e Boas Práticas da Universidade de Lisboa.

Acknowledgments

First of all, I would like to thank Professor João Torres for all his support and kind words since our first encounter in my second year till the end of this thesis.

To Ricardo Lameirinhas, a thank you is not enough to express my gratitude towards you for the whole of this project, your encouragement and help were fundamental to the development of this work. I wish you all the best, you great researcher!

To my parents, who always gave me wings to fly and a home to return to. Your help, advice, support and love was the motivation in the days I had none. Thank you. To my brother, who helps me see life in a lighter tone and still provides me guidance and support, thank you for your example.

A special thank you to my friends who have been by my side in these last few months, you believed in me even in the days I did not, you cheered me and kept me going. Thank you for the light hearted and the deep conversations, the laughs and the distractions from work.

Abstract

With the increasing interest in renewable energies, due to the rise in performances, the decrease in its prices and the increasing need for more sustainable solutions to power our societies, solar systems and especially photovoltaic systems have been an important asset. However, they present an almost counter-intuitive problem: in the peak hours of sun, their efficiency decreases due to the increase in temperature. In response to this problem, several systems have been designed using water, air and nanofluids as cooling agents. The main focus of this thesis is the cooling effect that happens to floating systems. This study was done experimentally, by setting up a floating system which comprises of two solar modules, one made of monocrystalline silicon and a CIGS one, floating on water. The water was cooled down using ice for some experiments in order to study the effects of the water temperature on the modules' performance. The effects of moving water was also studied.

Keywords

Efficiency; CIGS; Cooling Systems; Floating Systems;Monocrystalline Silicon; Photovoltaic Systems;

Resumo

Com o aumento do interesse por energias renováveis, devido ao aumento do desempenho, diminuição do preço e a crescente necessidade de soluções mais sustentáveis para a sociedade, os sistemas solares e especialmente os sistemas fotovoltaicos têm sido um recurso importante. No entanto, apresentam um problema quase contra-intuitivo: nas horas de pico do sol, a eficiência diminui devido ao aumento da temperatura. Em resposta a este problema, vários sistemas têm sido projetados usando água, ar e nanofluidos como agentes de arrefecimento. O foco principal desta tese é o efeito de arrefecimento que ocorre em sistemas flutuantes. Este estudo foi realizado experimentalmente, através da instalação de um sistema flutuante composto por dois módulos solares, um de silício monocristalino e outro CIGS, a flutuar em água. A água foi arrefecida com gelo para algumas experiências de forma a estudar os efeitos da temperatura da água no desempenho dos módulos. Os efeitos da água em movimento também foram estudados.

Palavras Chave

Eficiência; CIGS; Hibridização; Silício Monocristalino; Sistemas de arrefecimento; Sistemas flutuantes; Sistemas fotovoltaicos;

Contents

List of Figures

List of Tables

Acronyms

I_{SC} Short Circuit Current. 31, 32, 35, 37–39, 41

P_{max} Maximum Power. 41

V_{OC} Open Circuit Voltage. 29, 31, 32, 35, 37, 38, 41

1D One Dimension. 3, 43, 47

BIPV Building Integrated Photovoltaic. 23

CFD Computational Fluid Dynamics. 14

CIGS Copper Indium Gallium Diselenide. 3, 22–25, 33, 36, 39, 41, 43, 44, 46, 47

DC Direct Current. 11

FVM Finite Volume Method. 14

GC-CPCS Ground Coupled Central Panel Cooling System. 12

Mono-Si Monocrystalline Silicon. 3, 34, 36, 39, 40, 44, 46, 47

NASA North America Space Agency. 25

PCM Phase Change Materials. 16, 17

PV Photovoltaic. 2, 3, 8, 10–12, 16, 17, 23, 28, 46

SDG Sustainable Development Goals. 2

1

Introduction

Contents

1.1 Motivation

In the European Green Deal it is proposed by the European Commission to cut greenhouse gas emissions by at least 55% by 2030, which compels Europe to become climate neutral by 2050 - an economy with net-zero greenhouse gas emissions. In order to reach this goal more investment in Renewable Energy Sources must be made. Investment for their installation but also investment for their improvement. This fits into the United Nations Sustainable Development Goals (SDG), established on September 15, 2015 entitled as "Transforming our world: the 2030 Agenda for Sustainable Development". SDG have 17 agendas covering around 169 targets and are applicable to all the countries and regions of the globe. The goals in which Photovoltaic (PV) systems development fit are the 7^{th} - Affordable and Clean Energy, the 11^{th} - Sustainable cities and Communities and the 13^{th} - Climate Action [12].

Solar energy is crucial in the development of a more environmental friendly future. Over the years the average selling price of solar modules decreased 20% for each doubling of production volume, which was enabled by market conditions as well as technological advancements. PV systems' prices have followed the lowering price tendency of the solar modules but at a slower pace. The technical components of these systems share a global market, which allows for their prices to be similar globally (not considering taxes and duties). However, the price of the installed system varies significantly depending on is size, type of installation and country where it is installed, due to the legal requirements for permits, licenses and connection to the grid [13].This price lowering makes PV systems attractive for people to install in their houses for either home consumption or selling and injecting in the grid.

The first solar cell was developed by Charles Fritts in 1883 in New York when he coated selenium with a thin layer of gold. The conversion rate of this cell was 1-2%. The electric energy is produced through the photovoltaic effect, which converts the power transmitted in form of solar radiation to direct current using semiconductors. The photovoltaic effect is a physical phenomenon that occurs in the semiconductors when an adequate photon hits it, by the release of an electron-hole pair with the energy absorbed from the interaction. This effect is related to the conversion of radiative energy into electricity. The energy that is not converted to electrical energy is converted to thermal energy, which leads to the increase of temperature of the modules and consequently the reduction of their efficiency.

1.2 Objectives

The objective of this thesis is evaluating cooling systems already existing for solar panels. The main focus is dedicated to floating systems, as those are the ones more economically viable and which present overall more advantages. The study will focus on the comparison of two technologies and the influence of the temperature of the body of water in which the panels are installed as well as its stationary condition. This will be developed through experimental work performed in the laboratory using a Copper Indium Gallium Diselenide (CIGS) module and a Monocrystalline Silicon (Mono-Si) module. A One Dimension (1D) model for each technology will also be simulated in order to compare the baseline obtained experimentally with the simulation, to ensure the correct performance in the laboratory.

1.3 Outline

This document is divided into six chapters. The first one is an introductory chapter that explains the motivation for this work and the objectives it proposes to achieve. The second chapter presents some investigations done thus far towards the goal of reducing PV panels' temperature and several methods used to cool the PV systems will be analysed. Water, air and nanofluids based methods will be presented and the results of their studies will be shown and briefly discussed. Chapter 3 explains the technologies used to develop this work, their applications and market. In chapter 4 the experiments performed in order to evaluate the effect of the conditions of the water on floating systems are described, explained and their results are discussed and analysed. Chapter 5 shows brief simulations performed to compare the operation of the baseline case for both technologies used. The last chapter presents final conclusions extracted from this thesis and suggestions for future work are pointed out.

2

State-of-the-Art

Contents

2.1 Introduction

The photovoltaic effect is the creation of a voltage in a material after its exposure to light. When a photon of solar radiation containing enough energy hits an electron from the valence band, it moves to the conduction band, leaving a hole in its place, which behaves as a positive charge. Through the process of silicon doping, it is possible to create two layers in the cell, thus having a layer with an excess of positive charges and another with an excess of negative charges. In the region where the two materials meet, an electric field is created. By connecting the terminals to a circuit that is externally closed through a load, an electric current will circulate [1].

The photovoltaic cell is represented by its simplest model in Figure 2.1

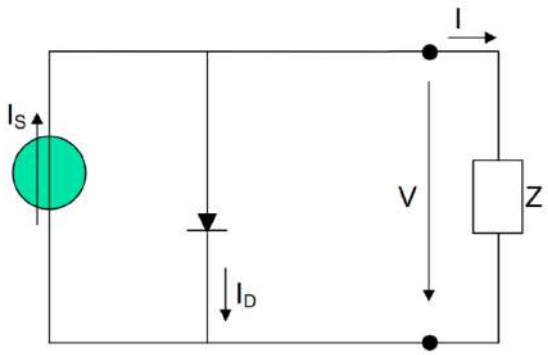

Figure 2.1: Equivalent circuit of a photovoltaic cell connected to load Z [1].

I_s is the current generated by the incident light. The diode represents the *pn* junction. Its current depends on the voltage *V* at the terminals and is given by:

$$I_D = I_0(e^{\frac{V}{mV_T}} - 1) \tag{2.1}$$

Where each term means:

- I_0: Diode maximum reverse saturation current
- V: Voltage at the terminals
- m: Ideal factor of diode. (m = 1 ideally, m $>$1 reallistically)
- V_T: Thermal voltage, which is given by $V_T = \frac{KT}{q}$
  - K: Boltzmann constant (K = 1.38×10^{-23} J/K)
  - T: Absolute temperature of the cell (in K)
  - *q*: Eletron electric charge ($q = 1.6 \times 10^{-19}$ c)

The current *I* that reaches the load is given by:

$$I = I_S - I_D = I_S - I_0(e^{\frac{V}{mV_T}} - 1) \tag{2.2}$$

Two working modes can be considered when working with PV systems: open circuit (*I* = 0) and short circuit (*V* = 0). These working modes give the open circuit voltage ($V_{OC} = mV_T ln(1 + \frac{I_S}{I_0})$) and short circuit current (I_{SC} = *I*), two important parameters to evaluate the performance of the PV panels.

These parameters and the remaining ones given by manufacturers are obtained under Standard Testing Conditions, which are cell temperature of 25℃, irradiance of 1000 W/m^2 and air mass 1.5. Irradiance and, consequently, temperature have the biggest impact on the solar cells and their efficiency. The temperature of the cell is given by the following expression:

$$T = T_{amb} + \frac{G(NOCT - 20)}{800} \tag{2.3}$$

Where:

- T_{amb}: ambient temperature
- *G*: Irrandiance
- *NOCT*: Normal operating cell temperature (temperature obtained by the cells in open circuit under STC conditions)

The influence of irradiance can be seen in Figure 2.2a and the influence of temperature can be seen in Figure 2.2b

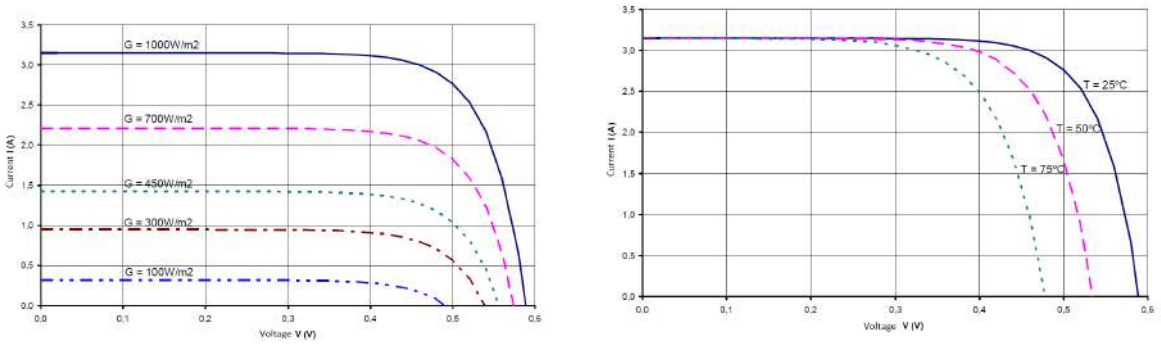

(a) Variation of I-V curve with irradiance.

(b) Variation of I-V curve with temperature.

Figure 2.2: Variation in I-V curves. [1]

The power output of a solar cell is therefore affected by the rise in temperature as can be seen in Figure 2.3.

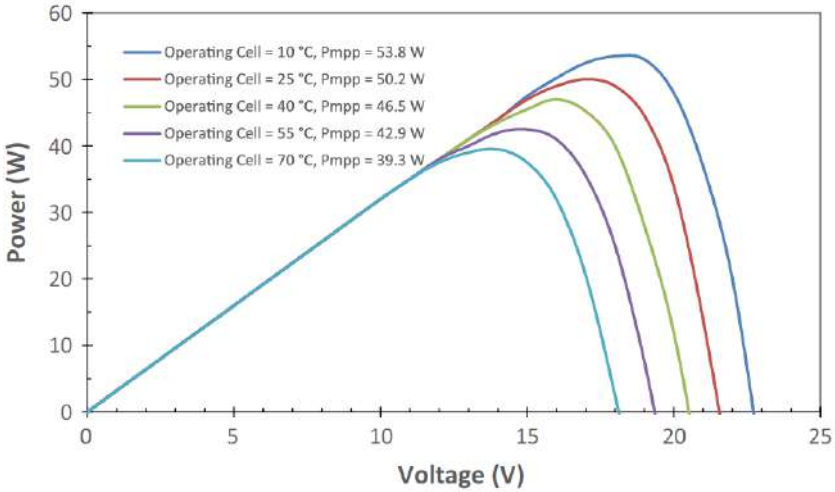

Figure 2.3: Variation of P-V curve with temperature [2].

The PV cells capture up to 80% of incident solar radiation but, however only a small fraction of the absorbed incident energy is converted into electricity, depending on the efficiency of the PV cell technology used. The rest of the energy absorbed by the PV cell is released as heat, and the it can reach a temperature of 40 degrees above ambient. [4]. This temperature increment leads to a decrease in the electrical output of around 0.4% to 0.65%, depending on the material, per every one degree increment in the operational temperature [14] [15].

Cooling methods have, therefore, been investigated in order to counteract this problem. They can be classified in two categories: active and passive. Active cooling systems are heat extraction mechanisms using devices such as fans or water pumps to extract away the heat (require energy) and passive cooling systems are technologies which reduce the temperature of the PV module by absorbing the heat from it without additional power consumption [16]. Mechanisms using air, water, phase change materials, desiccants and more have been designed and studied.

2.2 Water as cooling fluid

Water can be employed in several ways as a cooling fluid. Both active and passive systems can be developed and experimented. It is considered a better option for hotter regions due to water's high specific heat capacity and latent heat of vaporisation [17].

J. Siecker *et al* [3] studied a water spraying and a forced water circulation system. In the first, a centrifugal pump is used to force water flow through the spraying nozzles from a tank. The energy yield increases, but there is only partial cooling of the panel, which means that it is not an optimal system. In the latter, rectangular collecting pipes are mounted on the back side of the PV panel and water is

used as a circulating fluid, which allows the waste heat to be transferred to the circulating water (as can be seen in Figure 2.4) The electrical efficiency is increased and hot water can be utilised for domestic applications. However, this is a high cost system and optimal flow cannot be achieved in such a simple mode.

Figure 2.4: Hybrid solar Photovoltaic/Thermal (PV/T) cooled by forced water circulation [3].

In Figure 2.4 the numbers are:

- 1: PV modules
- 2: Circulation Pump
- 3: Water Storage Tank

In a similar setup as the last one mentioned, H. M. Bahaidarah *et al* [18] use an improved system by installing a flow meter to control the rate of the water flow. A maximum power point tracker (MPPT) was used to modulate the maximum power output and a controller with a smart tracking algorithm is used to provide load control to prevent overdischarge of the system's battery. This allowed for a reduction of 20% of the temperature of the panel and an increase of 9% of the electrical efficiency.

Mohamed R. Gomaa *et al* tested two systems, a flat photovoltaic/thermal system (PV/T) and a concentrating photovoltaic/thermal system (CPV/T), with water as a working fluid in order to improve their efficiencies. The CPV/T system uses linear Fresnel reflector mirrors as their concentrator system (as seen in Figure 2.5). TAt solar concentration ratio 3, the highest electrical energy produced rose from 65 W (at solar concentration 1) to 170 W. The highest amount of energy is produced at the highest flow rate of 1 kg/min under different concentration ratios. The temperature of the solar cells and absorber plate rises as the flow decreases. For example, when flow rate goes from 0.1 kg/min to 1 kg/min the temperature of the solar cells and the absorber plate reduces 22℃ and 28℃, respectively. The theoretical results show that the maximum electrical and thermal power outputs from PV/T module were 65 W and 170 W respectively, with cooling water flow of 1 kg/min. The maximum electrical and thermal

power outputs from CPV/T system were 170W and 580W respectively, at solar concentration ratio 3 and cooling water flow of 1 kg/min. The experimental results confirm the tendency and show that the maximum electrical and thermal power outputs from PV/T module were 60W and 185W respectively. The maximum electrical and thermal power outputs from CPV/T system were 130W and 525W respectively, at solar concentration ratio 3, cooling water flow 0.7 kg/min and 900 W/m^2 solar irradiance. The total power of the PV/T module was 245W and the CPV/T system was 655W, with power increasing 167%. [4]

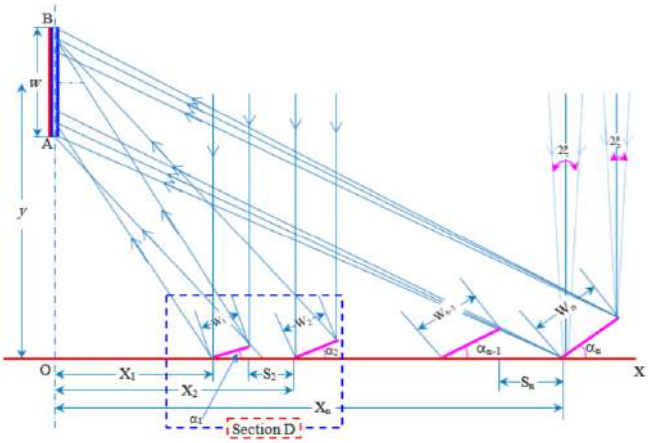

Figure 2.5: CPV/T system [4].

In Figure 2.5, the inclined pink lines on the bottom represent the concentrating mirrors and the blue elevated line on the top left corner represents the solar panel.

V. Sílva *et al* tested a cooling system that consists of a water film on the front face of the panel. The tests took part in several seasons of the year under different climatic conditions, in order to understand the panel behaviour. The best performance of the cooling system happened during the summer, with a maximum temperature reduction of 35% (21℃) and a maximum energy gain of 9.3%. The average temperature reduction was 18% (8℃) in this season. The worst registered season was the autumn, however the average reduction of temperature was still 15% (7℃) and the average energy gain was 5%. It was noted that the continuous operation of the water-film caused incrustation of a thin white crust on the top surface of the module, which caused its efficiency to decrease [19].

2.3 Air as cooling fluid

Air can be employed in several ways to serve as a cooling agent for PV modules.

J. Siecker *et al* [3] studied an hybrid solar Photovoltaic/Thermal system cooled by forced air circulation as seen in Figure 2.6. In this system a Photovoltaic module is set on top of a steel plate with an air channel underneath it. The air is forced through the channels by a fan with a nozzle, which is powered by

the PV module. The heat is transferred from the panel to the air via convection. This system was found to be economically viable and it improved the overall efficiency of the module. The hot air extracted from the PV can be used to heat indoor spaces in case the system is installed in buildings. This system is most effective in colder climates, given that in hotter ones the temperature difference between the panel and the air is not big enough to allow for convection.

Figure 2.6: PV/T system cooled by forced air circulation [3].

Where:

- 1: PV modules
- 2: Forced circulation fan
- 3: Air channel

Z. Farhana *et al* [5] tested a system comprising of a DC brushless fan and a heat sink fitted underneath a PV module as seen in Figure 2.7. The heat sink, made of aluminium, is used to distribute the heat generated and increase the heat transfer rate. With the cooling system implemented for every 100 W/m^2 increase in the incdent solar radiation, the temperature of the panel increased 1.6 ºC. Without the cooling system this increase is 1.8 ºC. This system allowed for a maximum of 12 ºC decrease, equivalent to 40% decrease in the panel temperature. These results, however, require some verification given that the temperature difference is so little (0.2 ºC) that it could be attributed to the error of the measuring device.

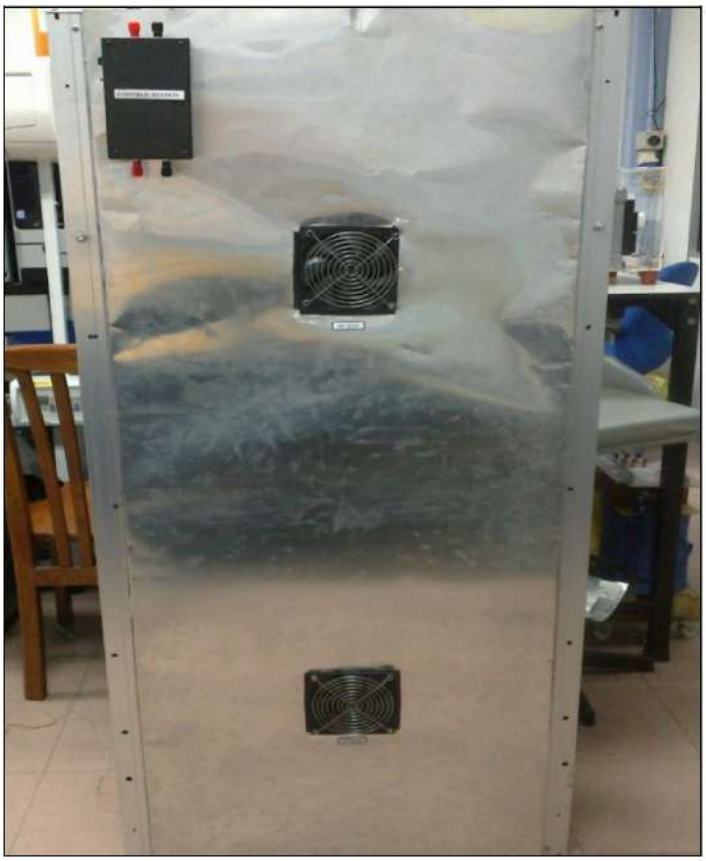

Figure 2.7: Backside of the panel with the fan and the heat sink [5].

M. Hasanuzzanan *et al* [2] tested a conventional passive cooling system in which the modules are cooled by radiation and free convection. They claim that adding a channel at the back of the PV panels drops their temperature by up to 20º C with a subsequent gain of 1 to 2 % in overall efficiency. An active cooling system: a Ground Coupled Central Panel Cooling System (GC-CPCS), which served the solar panels by forced convection of air driven by a blower, blower which was run by a dedicated panel. The air flows through a ground-coupled heat exchanger and decreases its temperature. The cooled air soothes the solar panels while passing beneath them [20]. The effects of the air gap size and the effects of free and forced ventilation through various geometries of ducts is studied.

J. Wajs *et al* [6] sudied the cooling of a PV roof tile by placing it in a specially designed wooden casing (Figure 2.8) that formed a channel through which the air flowed, cooling the back wall of the tile. In the laboratory the air was forced to flow using a radial fan to reproduce the natural conditions. It is to be noted that wind speed is the key to obtain good results when using this technique.

A maximum increase of 9.5% in electrical efficiency was found for solar irradiance of 600 W/m^2. The maximum overall efficiency obtained was 23.5% at a solar irradiance of 900 W/m^2.

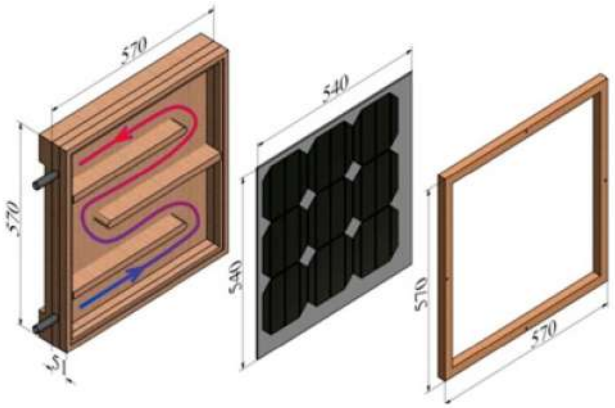

Figure 2.8: 3D model of the of the PV roof tile casing [6].

The usage of air as a coolant is cheap and simple, however, it provides better results in ambient temperatures below 20℃ [17].

2.4 Nanofluid as cooling fluid

Nanofluids are colloidal solutions that are obtained by dispersing nanoparticles in a base fluid, which leads to an enhancement of the thermal and electrical efficiency compared to simply the base fluid. This is due to an improvement of the heat transfer coefficient between the tube where the nanofluid circulates and the fluid itself [21].

M. I. Hussain *et al* [22] designed a dynamic model for a dual fluid Photovoltaic/Thermal (PV/T) system that uses a nanofluid and air simultaneously. The first step consisted of identifying the optimal nanofluid type by dispersing metal oxide nanoparticles such as copper oxide (CuO), aluminum oxide (Al_2O_3) and silicon dioxide (SiO_2) with diferent concentrations in the base fluid. The optimal centration was found to be 0.75% in water for CuO, as it has a lower specific heat and a slightly higher thermal conductivity. The nanofluid and air are forced to circulate in copper tubes and an air duct, respectively, both independently and simultaneously, according to the system's design. The modelling and numerical analysis were performed based on the following steps:

- 1: Develop a dual fluid PV/T model;
- 2: Assess the thermal performance of the collector under various conditions;
- 3: Validate using experimental data.

The continuous governing equations were discretized using a Computational Fluid Dynamics solver based on the Finite Volume Method.

In order to discover the optimal flow rate of each of the running fluids, both were operated independently while the other is kept stagnant. The increasing of the flow rate of both fluids increases the efficiency. The impact of increasing the flow rate of the nanofluid is bigger than that of the air due to its better thermal properties and high heat removal capability, so the nanofluid flow rate is varied and the air's was kept constant.

In another study, O. Rejeb *et al* [7] did an experimental and numerical study to evaluate the performance of a PV/T nanofluid based collector. The influence of concentrations, types of nanoparticles and base fluids on the electrical performance was tested in three different cities: Lyon (France), Mashhad (Iran) and Monastir (Tunisia). The setup used is shown in Figure 2.9. The tested base fluids are water and ethylene glycol (EG). Aluminum oxide (Al_2O_3) and copper (Cu) are tested as nanoparticles. It is noted that water yields a better result as a base fluid and after further testing, the combination of water and copper offers the best efficiency results, which are 13.55% electrical efficiency and 76.88% thermal efficiency. These results were obtained for Monastir due to its highest average solar radiation, which yields an electrical and thermal output of 285 kWh/m^2 and 791 kWh/m^2, respectively.

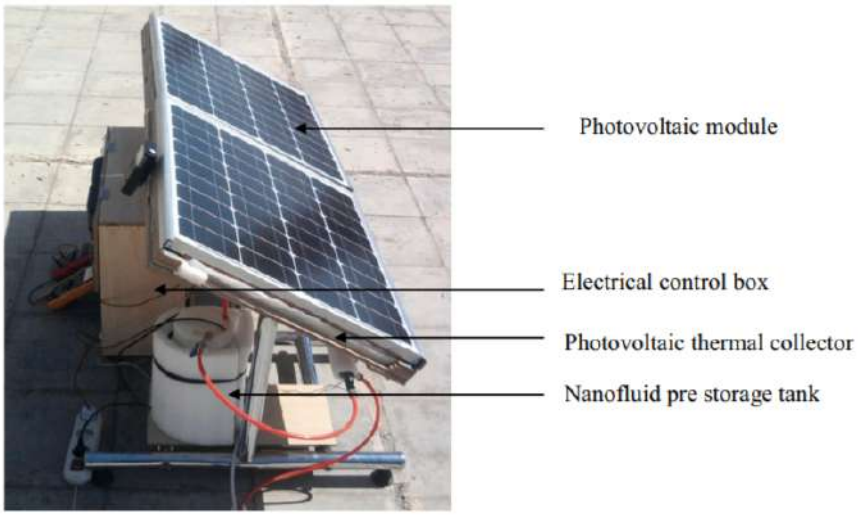

Figure 2.9: Experimental setup for PV/T nanofluid based collector [7].

2.5 Floating Technology

Floating solar systems are a new way of implementing solar farms. Instead of the traditional rooftop or ground mounted systems, these are installed on large bodies of water such as the reservoirs of

hydroelectric power plants, lakes, and under the right conditions, oceans. A report by Wood Mackenzie, a global research firm, argues that global floating solar demand is expected to grow by an average of 22 percent year-over-year from 2019 through 2024 [23].

Figure 2.10: Floating System in Alto Rabagão dam reservoir, Montalegre, Portugal.

An important benefit to floating technology is that no land is occupied. This land is valuable either for wild life, farming or construction. Reduced grid interconnection costs are also an advantage to these systems. Installing a new energy source where energy is already being injected into the network, called hybridization, allows for savings (due to the reduced infrastructure needed to be installed in order to achieve the goal of injecting this energy in the grid) and for the increase of the duration of the power supply [24].

Furthermore, these panels do not suffer from shading from buildings or other infrastructures near them, which allows for a better performance.

Another benefit, and the most relevant one for this dissertation, is the cooling effect that having these panels on a water surface brings. As seen previously, water is a very good cooling fluid due to its high specific heat capacity. Allowing the whole surface area of the panel to be in close contact with water can reduce the panel's temperature up to 5-10% [25] [26]. These values need further studying and investigation, given that this is a very recent technology, thus not much data is yet available nor many studies have been done on concrete cases and not only on hypothesis and simulations.

These systems however, present some challenges which drive their prices up and are still in need of better developing and research. Anchoring and mooring the giant platforms that sustain the panels are a big part of the cost of these systems. Another consideration is the moving parts that are subject to constant friction and mechanical stress: systems that are poorly designed and maintained can suffer from catastrophic failures. The risk of degradation and corrosion due to moisture also increases in this scenario [25].

The environmental impact on the quality of water and on the wildlife are also prime concerns of this technology [27] and still lack deeper studying in order to understand the concrete implications.

These systems are present in Portugal in Alto Rabagão dam reservoir as seen in Figure 2.10 with 840 panels and an installed power of 220 kW and in Alqueva dam reservoir (see Figure 2.11) with an installed power of 4 MW [28]. In Alqueva more than 12,000 panels are to be installed, with an annual installed capacity of 7 GWh. This farm also includes a new system of batteries and energy storage. It is a perfect example of the hibridization of energy technologies. Another advantage of this common environment is the usage of the solar energy in the periods of lower consumption to pump back the water in the dam in order to reuse it to produce hydroelectrical energy. It is predicted that this system will provide energy equivalent to the consumption of 25% of the consumers in the region [29]. It is predicted that the floating farm will start producing energy by the end of 2021.

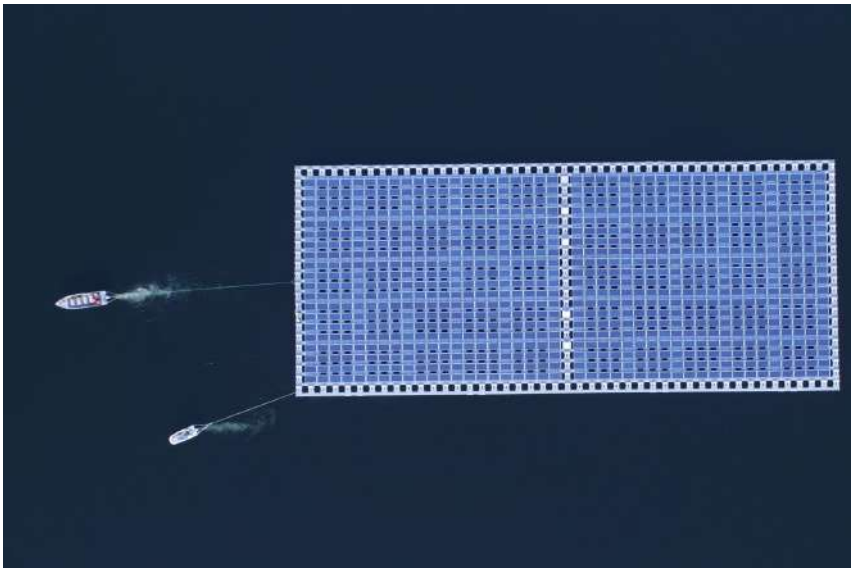

Figure 2.11: Installation of floating System in Alqueva reservoir, Portugal.

Overseas, in Singapore lies the largest floating solar farm in the Tengeh reservoir (see Figure 2.12) , with an installed power of 60 MW, made up of 122,000 solar panels spanning 45 hectares [30]. During the pilot tests, there was a 15% increase in the performance of the solar system when compared to a conventional rooftop system. Due to this success, two more floating solar farms are being planned to be completed this year in Singapore.

2.6 Other cooling methods

Other methods have been studied in order to improve the PV panels' efficiency, including, but not limited to, Phase Change Materials, Desiccants and Thermoelectric Modules.

Figure 2.12: Floating System in Tengeh reservoir, Singapore.

Phase Change Materials (PCM) are materials that when the temperature increases, as an endothermic process, they absorb the heat and the chemical bonds separate and the material changes phase from solid to liquid. When the melting process is complete, the temperature stabilises [31].

P. Singh *et al* studied three polycrystalline silicon-based roof integrated PV systems in which one was the reference, one was had a PCM container in the back of the panel and the other had PCM and fins. The PCM container was made of aluminum and the PCM chosen was paraffin wax. The schemes of the studied systems are shown in Figure 2.13.

The peak temperature of the systems were 45.15℃, 31.55℃ and 25.95℃ for system one, two and three, respectively. This shows that the fins enhance the heat transfer from the PV to the PCM. The peak power production happens at 12 PM and it is 2551W, 2770W and 2816W for system one, two and three, respectively and consequently the electrical efficiency is 13.23%, 14.11% and 14.45%. However, the finned PCM system is not deemed economical due to its cost of power production (higher than that of the reference system). These systems were tested in the Southeast of England and the main reason for this bad result is the number of rainy/cloudy days, which render the PCM unused.

Apart from that, PCM have low efficiency in cold climates, proving to be better for hotter climates [3].

Desiccants are an hygroscopic substance that is used to induce or sustain a state of dryness in its vicinity. The aim of L. J. Simpson *et al* was to integrate material on the PV module that absorbs water from the air at night (when the PV temperature is low and the relative temperature is high) and when this water evaporates during the day it should remove the excess heat and consequently reduce the PV module temperature [9]. The illustration of this idea is present in Figure 2.14.

Several materials were studied for this application, both liquid and solid-based. Liquid desiccants require a container to allow for water vapour to pass in and out while retaining the liquid inside. Solid desiccants need to be integrated in the module while still having access to the air. An hygrothermal

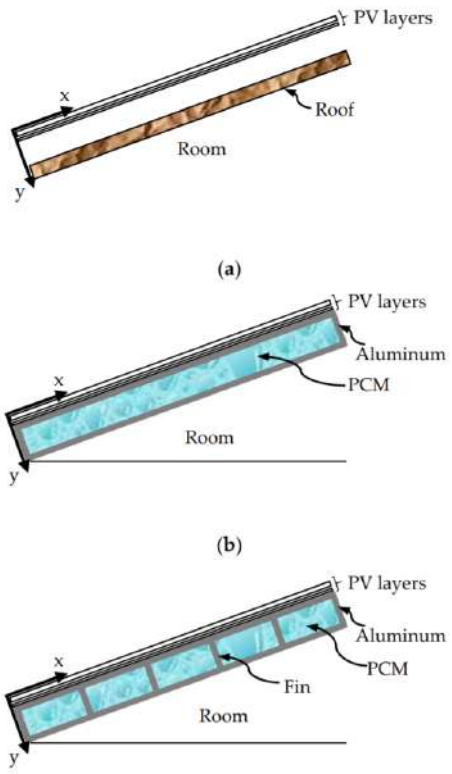

Figure 2.13: Scheme of the studied systems: a) PV reference system; b) PV-PCM system; c) PV-finned PCM system [8].

model was developed to validate the concept and it predicts a peak cooling of 8℃ with $LiCl$ (Lithium Chloride).

Another system studied consists of the integration of a thermoelectric module operating in Peltier mode under the back of the solar cell (Peltier Module). Another thermoelectric module is attached to the underside of the the Peltier Module working in Seebeck mode (Seebeck Module). When a junction of two types of materials (n and p) is subjected to an electric current, heat is absorbed. A thermoelectric material will generate cold or heat when applied an electric current [32]. The ratio of the heat emitted and the current applied is given according to Equation 2.4 and it is called the Peltier Coefficient (π_{AB}).

$$\pi_{AB} = \frac{dQ}{dI} \tag{2.4}$$

The Seebeck Effect happens when an electrical voltage appears at the junctions of two different types of materials (n and p) subjected to a temperature difference. The ratio of the voltage generated and the temperature difference is given by the Seebeck Coefficient (S) and is expressed in Equation 2.5.

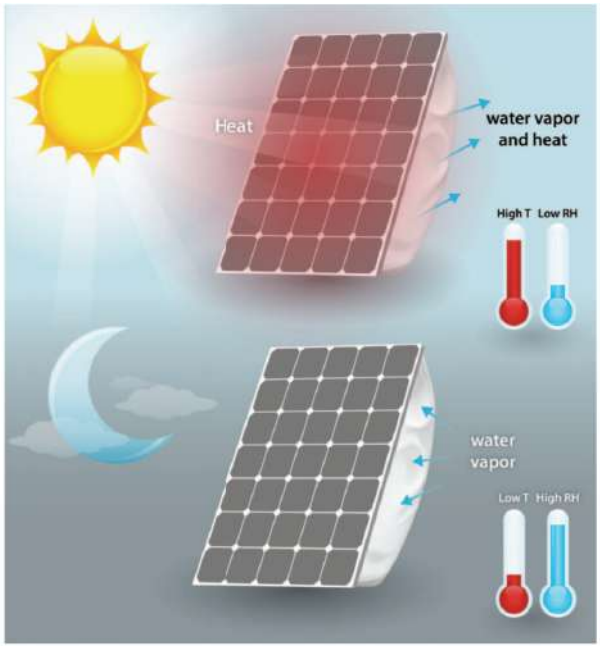

Figure 2.14: Illustration of the use of desiccants [9].

$$S = \frac{\Delta V}{\Delta T} \tag{2.5}$$

A schematic of the system described is presented in Figure 2.15 where TEC means thermoelectric cooler and TEG means thermoelectric generator.

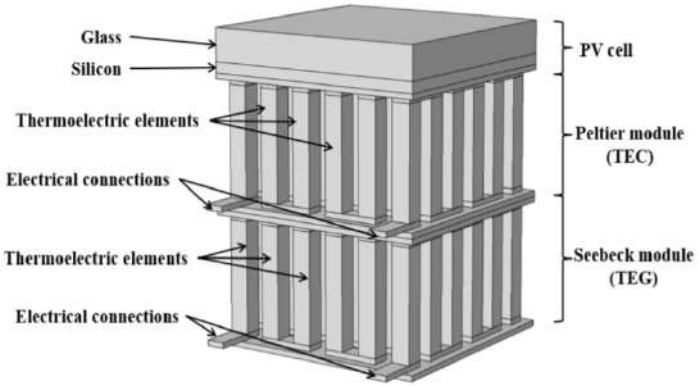

Figure 2.15: Schematic of the hybrid system configuration [10].

When the temperature of the cell increases the TEC will cool it when a current is applied to it. The TEC will transmit the heat absorbed from the panel to the TEG which, in its turn, will generate additional electrical power. At a temperature of 40ºC the power output is 2.5W. When connected to the TEC module

the temperature reduces to 37℃ and the power output increases to 2.54W. After connection to the TEG module the power output increases to 2.6W.

3

Solar Cell Technologies

Contents

3.1 CIGS

Copper Indium Gallium Diselenide $CuIn_{(1-x)}Ga_xSe_2$ - CIGS - is a semicondutor that varies its band gap value between 1.0 - 1.7 eV depending on the proportion of its elements [33] [34]. It can originate thin film solar cells, which are composed by 6 (six) layers, from the top to the bottom, as can be seen in Figure 3.1 [35]:

- Transparent front contact of aluminium doped zinc oxide - **Al-ZnO**
- A thin layer of highly resistive undoped zinc oxide - **I-ZnO**
- n-type buffer layer of cadmium sulphide **Cds** *or* zinc oxy sulphide - **Zn(O,S)**
- p-type absorbing layer consisting of copper indium gallium diselenide - **CIGS**
- metallic molybdenum back contact - **Mo**
- soda-lime glass

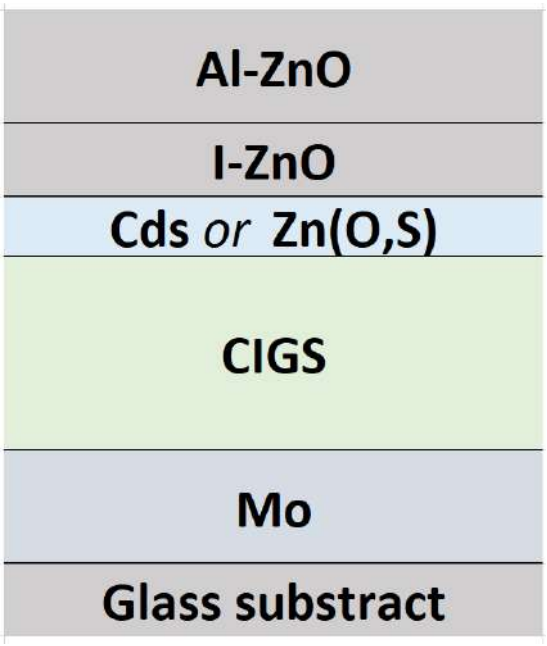

Figure 3.1: CIGS cell model (levels not at scale).

CIGS are considered 2^{nd} generation technology. The 1^{st} one is based on crystalline silicon technologies, both monocrystalline and polycrystalline, and on gallium arsenide (GaAs); the 2^{nd} generation includes amorphous silicon (a-Si) and microcrystalline silicon (μ-Si) thin films solar cells, cadmium telluride/cadmium sulfide (CdTe/CdS) and copper indium gallium selenide (CIGS) solar cells; the 3^{rd} generation involves technologies based on more recent compounds such as nanocrystalline films, active

quantum dots, tandem or stacked multilayers of inorganics based on III–V materials, such as GaAs/-GaInP, organic (polymer)-based solar cells and dyed-sensitized solar cells; lastly, the 4^{th} generation combines the low cost and the flexibility of polymer thin films with the stability of novel inorganic nanostructures such as metal nanoparticles and metal oxides or organic-based nanomaterials like carbon nanotubes, graphene and its derivatives [33] [36].

The increase of temperature affects CIGS panels the same way it affects every other technology: reducing its efficiency. However, in high solar incidence days, which result in high surface temperatures, CIGS panels exhibit higher energy yield values than polycrystalline ones [11].

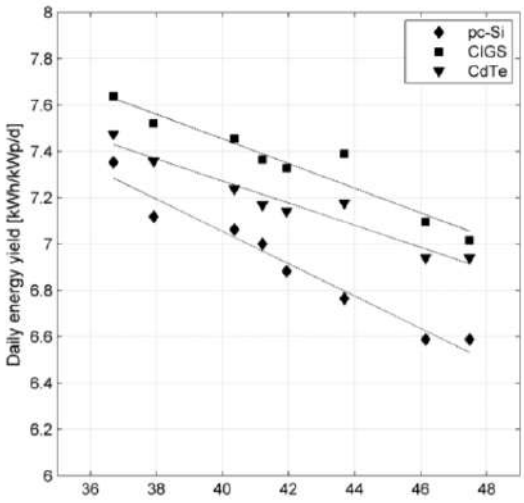

Figure 3.2: Daily energy yield vs daily average temperature of different technologies for sunny summer days [11].

This is due to a lower temperature coefficient than in the case of polycrystalline modules and higher power gains due to spectral effects, which are more remarkable at high latitudes in the north hemisphere as reported by Daniela Dirnberger *et al* in [37].

In 2014 an efficiency record of 21.7% had been obtained by The Centre for Solar Energy and Hydrogen Research Baden Württemberg (ZSW) [38]. This is, however, very experimental and academic, not being replicated for real life modules yet, which means, no solar panel with this efficiency has been produced for public market yet.

3.1.1 Applications and Market

The current market for Photovoltaic solutions is composed of mostly first and second generation technologies [33]. CIGS technology, however, is expanding its presence in the solar panels market due to their low temperature coefficient and high absorption capability in the ultraviolet and infrared zones of the light spectrum. One way of inserting this technology into our societies is through Building Integrated Photovoltaic (BIPV) systems. The thin film technology presents itself as the future of this technology due

to the low weight, flexibility, suitability for vertical installation and affordability [39]. The vertical installation allows for curtain walls to be created, which increase the exposed area and decrease the visual pollution that some solar installations cause. In the South Railway station in Beijing, China a roof mount approach was chosen (Figure 3.3), having had installed 5200 CIGS modules, which amount to 435 kWp of installed capacity.

Figure 3.3: South Railway Station, Beijing, China.

Another example of a BIPV system with the use of CIGS panels is in the Godsbanen Cultural Center in Aarhus, Denmark.

Figure 3.4: Godsbanen Cultural Center, Aarhus, Denmark.

On the other hand, space technologies are a promising receptor of this technology. The low weight, specific volume and mechanical reliability are characteristics that make CIGS technlogy a good bet in space exploration [40]. The CIGS panels from the company Ascent Solar have been undergoing several extensive evaluations by North America Space Agency and in November 2018 were sent as a part of the 10th Materials International Space Station Experiment (MISSE-X) flight experiment aboard the International Space Station [41].

3.2 Crystalline Technology

Monocrystalline silicon (Mono-Si) is the base material for silicon-based discrete components and integrated circuits used in virtually all modern electronic equipment. It can also be employed as a light-absorbing material in the production of solar cells, which is the application investigated in this research.

Figure 3.5: Monocrystalline Silicon cell.

Monocrystalline silicon is obtained from a block of a monocrystal of pure silicon. The monocrystaline silicon cells can be produced following the next steps [42]:

- Preparation of the silicon surface - this includes degreasing and cleaning the silicon wafer surface;
- Formation of the *pn* junction by diffusion of dopant donor to the base wafer (type p);
- Junction insulation and phosphorous-silicate glass removal;
- Surface passivation, which significantly reduces velocity of the surface recombination;
- Anti reflection coating deposition (TiO_x) in the front of the wafer;
- Formation of metal contacts - these should have ohmic contacts with silicon, low contact resistivity and good adhesion to silicon.

As previously stated, silicon based technologies are first generation technologies and have the biggest market share in photovoltaic technologies.

3.2.1 Applications and Market

Monocrystalline silicon cells present a higher production cost when compared to polycrystalline modules, but they also present higher efficiency. As a consequence, a smaller area of silicon is needed to produce the same amount of energy. This is the reason why they are primarily chosen for solar systems in rooftops, and for small systems that need power, such as traffic lights, velocity sensors, *etc* (Figure 3.6). They are also employed in big solar parks which aim at providing the general grid with energy, due to their high energy yield. For this latter option, new systems are being tested and employed, such as bifacial solar modules, which take advantage of the light reflection on the ground.

Figure 3.6: Monocrystalline Silicon cell used in an SOS post in Portuguese highways.

Figure 3.7: Bifacial monocrystalline solar modules.

Monocrystalline silicon modules represented about 35% of market share in 2011 according to Professor Rui Castro in his book ”Uma Introdução às Energias Renováveis: Eólica, Fotovoltaica e Mini-hídrica” [43]. More recent data shows that in 2020 Mono-Si modules represented about 75% of the market share and it is predicted to keep growing [44] [45].

4

Experimental Work

Contents

4.1 CIGS Experiments

The specific panels used to perform the following experiments are from the brand Hanergy, the model is SC-8GUR and its technical specifications are as shown in Table 4.1:

Power [W]	7.7
Output Voltage [V]	5
Peak Output Current [A]	1.2

Table 4.1: CIGS modules specifications.

They are similar to the ones in Figure 4.1:

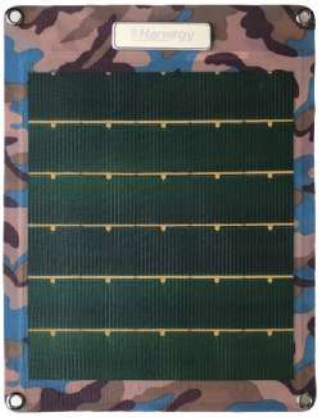

Figure 4.1: CIGS panel used to perform the experiments.

4.1.1 Establishing a base line for comparisons

Starting at room temperature, two I-V curves were obtained. The difference between them lies at the height at which the lamp was. The first experiment was performed at an height of 30 cm and the second one at an height of 15 cm. The lamp used was a 200 W incandescent Philips lamp and the area of the panel is 0.05184 m^2.

The increase in radiation shows the increase of the I_{SC}, which was to be expected as seen in Figure 2.2a. Also, the current in the PV panel can be described as in Equation 4.1 where *A* is the area of the module and G_{fe} is the photoelectric generation. This further explains why lowering the lamp increases the short circuit current.

$$I_{PV} = A \times Gef \tag{4.1}$$

The I-V curves resulting of these experiments can be seen in Figure 4.2a and the corresponding P-V curves can be seen in Figure 4.2b.

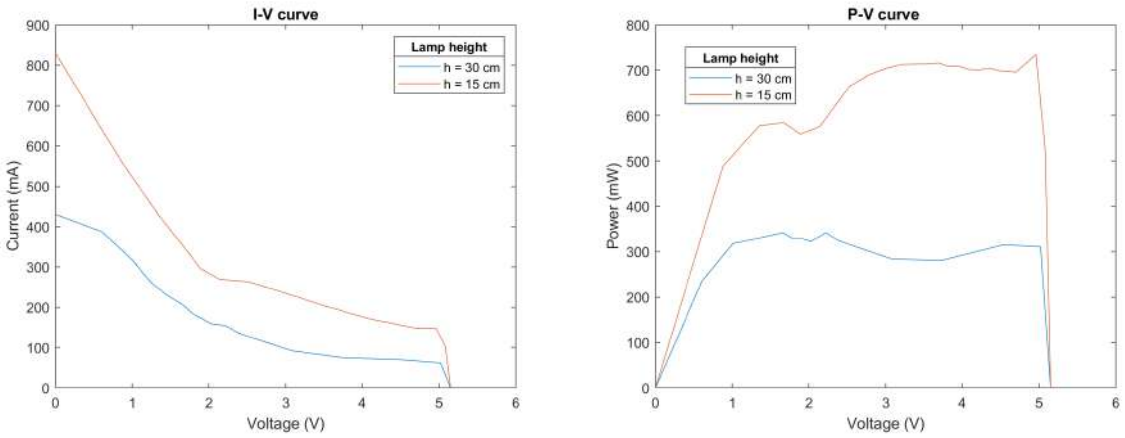

(a) I-V curves.

(b) P-V curves.

Figure 4.2: CIGS: baseline - experimental results.

By lowering the lamp, the irradiance increases and consequently, so does the temperature of the panel. In the second experiment, which took around 10 minutes to perform and the lamp was constantly turned on, there was an increase of 6 ℃ of the surface temperature of the module. It is expected that this temperature would keep increasing for as long as the experiment was running, *i.e.*, as long as the lamp was turned on (considering that the experiment is performed in a reasonable amount of time which does not allow for the module's temperature to reach its peak). Although there was a temperature increase in the first experiment, it was not as significant as in the last one. However, given the relatively short duration of these experiments, no alterations can be seen in the V_{OC} as would be expected.

The experimental setup is shown in Figure 4.3:

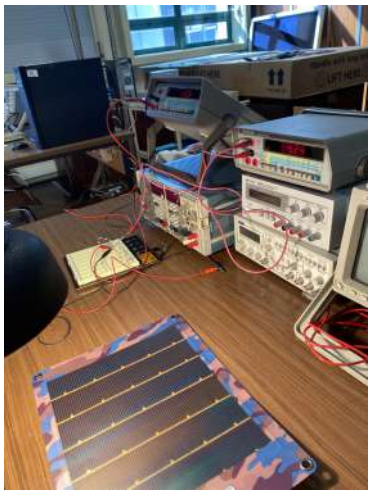

Figure 4.3: Experimental setup to obtain the baseline I-V curves of the CIGS module.

4.1.2 Floating experiments

Experiments were carried out to better understand the alterations that floating on water causes to the panels. In order to emulate the water of a dam reservoir, a plastic box containing water was used. Since in real life conditions, the panels do not touch the water directly, two floats were employed, one on each end of the module, to prevent it from touching the water (see Figure 4.4). There was also the goal of having as little material as possible between the water and the module that would impair the heat conductivity.

Figure 4.4: Floats used to help the floating of the CIGS module.

4.1.2.A Fresh water at room temperature

The lamp in this experiment was placed at a distance of 15 cm from the solar module. The I-V and P-V curves were obtained, as well as the temperature of the module during the experiment. The water was at room temperature, and at this point there was no attempt of either cooling or heating it.

The setup of this experience is shown in Figure 4.5.

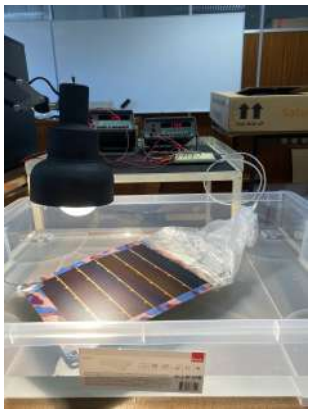

Figure 4.5: Experimental setup to obtain the baseline I-V curves of the CIGS module.

In this experiment, it is expected that the I_{SC} will remain roughly the same if not slightly higher, because of the light reflection on the water. The V_{OC} will not decrease significantly since the module temperature will not increase as much compared to the previously established baseline.

The resulting I-V and P-V curves are presented in Figure 4.6:

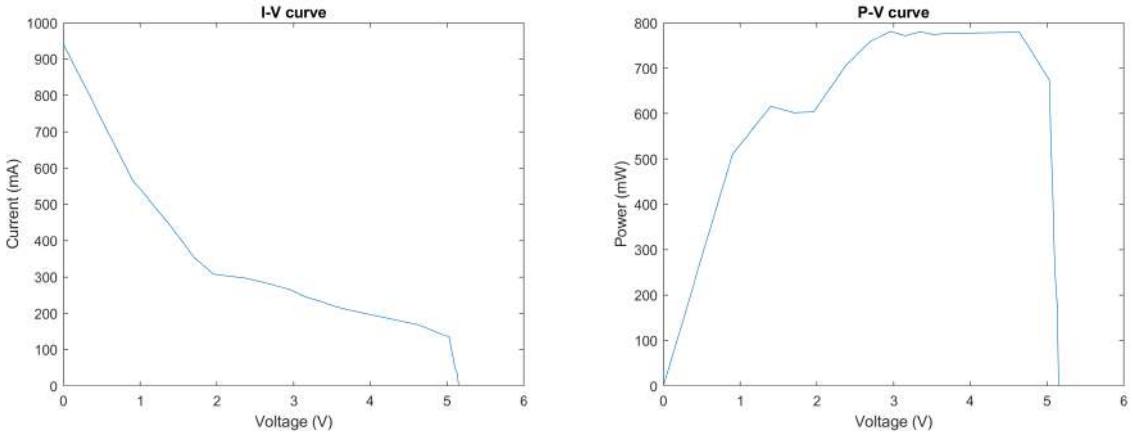

(a) I-V curve. **(b)** P-V curve.

Figure 4.6: CIGS: floating in fresh water at room temperature - experimental results.

Comparing the findings of this experiment to those obtained for the same irradiance, that is, when the lamp was positioned 15 cm above the solar module, the I_{SC} increased approximately 100 mA, while the V_{OC} remained the same. Since both experiments took the same amount of time to perform, it can be inferred that floating modules can provide more current, as one would anticipate.

For the 10 minutes it took to perform this experience, the temperature of the module rose 5 ℃ for the first 5 minutes and then it stabilised for the rest of the experiment. Extrapolating this information for real life conditions, it means that panels on floating conditions, will see their temperature increase just up to certain threshold, which will then stabilise. This means that the panels will not reach such a high temperature that will impair their functioning and efficiency, allowing for a bigger energy yield for the same amount of time as a system with the same specifications but mounted on the ground or in a rooftop.

4.1.2.B Fresh water cooled by ice

In order to analyse the effect that the water temperature has on floating systems, in the same setup as used previously, 4 kg of ice were added to the water. The I-V and P-V curves were obtained for the following water temperatures:

- **8.5 ℃**: the ice had been added a few minutes ago and it was still melting;
- **5.5 ℃**: the ice had just finished melting, the water was at its coldest temperature;

- **6 ℃**: the water was starting to increase its temperature.
- **7 ℃**: the water was increasing its temperature.

It is expected that the colder the water, the higher the I_{SC}, as the temperature of the solar cells is not going to increase as to hinder the conversion efficiency.

The results of the experiment are shown in the following Figure 4.7:

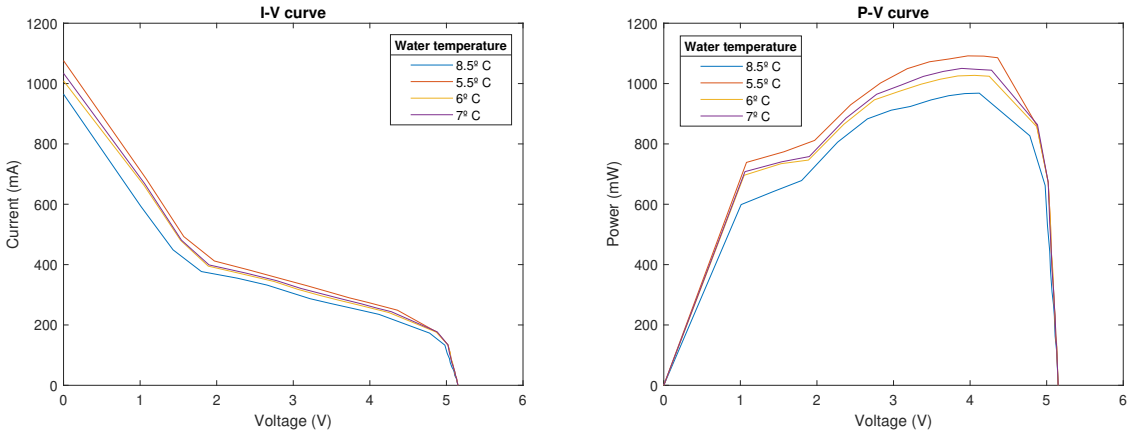

(a) I-V curves.

(b) P-V curves.

Figure 4.7: CIGS: floating in fresh water cooled by ice - experimental results.

According to the previous graphs, the colder the water, the higher the value I_{SC}. Provided that the V_{OC} remains the same, the output power increases with the decrease of the water temperature, as was predicted. This means more energy extracted for the same amount of time which translates into better efficiency. A table summarising the temperature increases for each experiment performed is present in section 6.1.

Colder climates could benefit more from floating systems since the waters in lakes and reservoirs are at colder temperature.

4.1.2.C Emulating waves in fresh water

Taking into account that under some very specific conditions floating parks can be installed in seas and not only lakes or reservoir dams, there was a need to study whether the movement of water had any effect on the performance of the solar modules.

The experimental setup is similar to the previous experiments: fresh water in a plastic box and the module set on floats at a distance of 15 cm from the lamp. In order to emulate waves, an electric mixer was used.

The results obtained in this experiment can be seen in Figure 4.8:

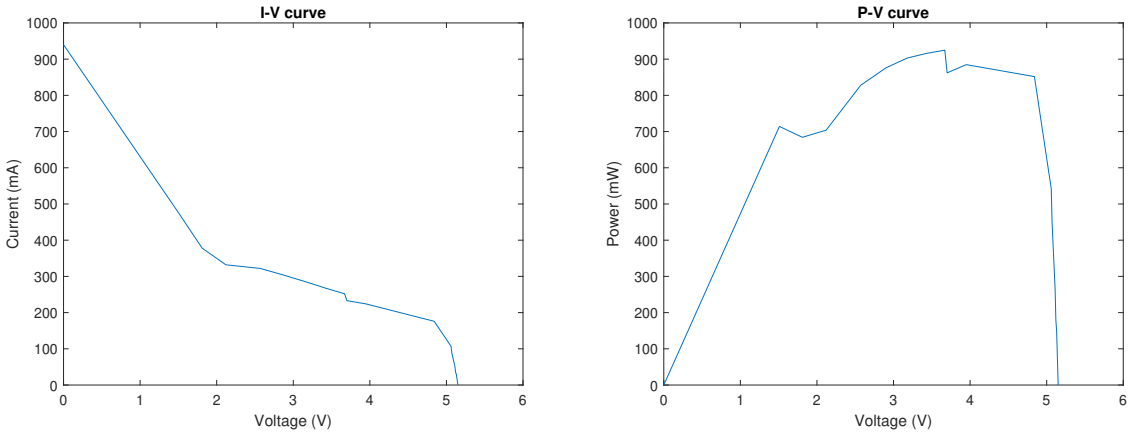

(a) I-V curves.

(b) P-V curves.

Figure 4.8: CIGS: emulating waves in fresh water - experimental results.

In this experiment there was only a 1.5 ℃ increase in the module's temperature. This can be explained due to the ambient temperature being low on this day when compared to the previous experiments and due to the splashes of water that fall on the top of the module. Instead of the cooling being only done on the backside as in previous experiments, in this case cooling also happens on the front side, which prevents the temperature from rising as much. In the short run, this is a positive factor because it stops the module's temperature from rising, however in the long run it may have detrimental effects, as after the deposed water evaporates, foreign substances will be settled on the front of the panel, causing hotspots and in the longer run it may corrode and damage the front side of the panel altogether. This can be avoided with frequent cleaning and maintenance of the panel, although this brings extra costs which may exceed the value of the extra energy produced.

Due to the movement of the water and the constant rocking of the modules, which affects the angle at which light reaches the module and, as a result, its absorption and energy conversion, these curves are not as smooth as the previous ones.

4.1.2.D Emulating waves in fresh water cooled by ice

It was now necessary to evaluate the influence of the water temperature in potential solar farms installed in the seas using CIGS technology, where there is constant water movement. For this experiment, 4 kg of ice were added to the fresh water in the box as previously done and the waves were emulated with the electric mixer, as done in the last experiment.

The operating curves were obtained for the following water temperatures:

- **1.2 ℃**: the ice had just finished melting, the water was at its coldest temperature;
- **5.5 ℃**: the water temperature was increasing, this was similar value to one obtained previously,

which allows for a good comparison.

The I-V and P-V curves can be observed in Figure 4.9a and Figure 4.9b, respectively.

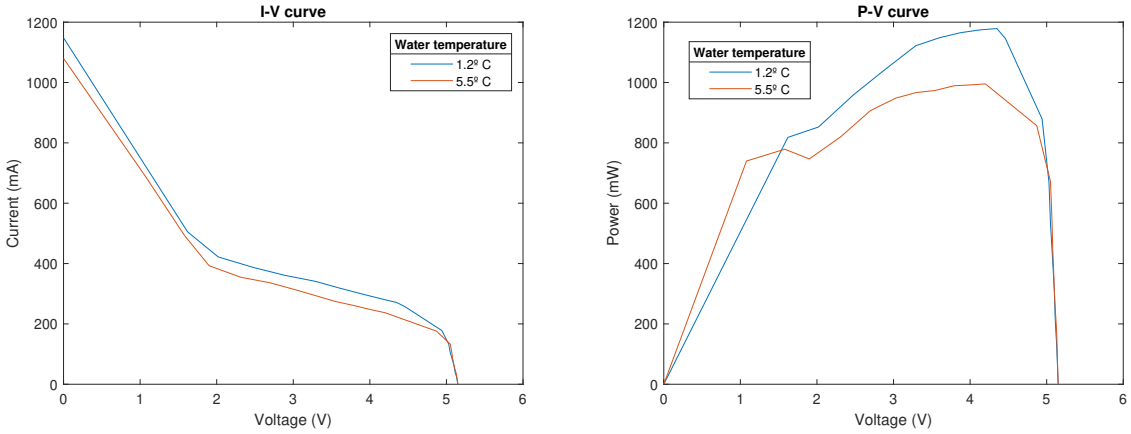

(a) I-V curves.

(b) P-V curves.

Figure 4.9: CIGS: emulating waves in fresh water cooled by ice - experimental results.

For the coldest water temperature registered, the solar module only increased its temperature by 0.5 ℃. This is a very low value and it gets the module near its top performance. When the water reached 5.5 ℃, there was an increase of 1 ℃ in the module's temperature. Comparing this value to the one obtained in Section 4.1.2.B, in which there was an increase of 1.5 ℃, it can be ascertained that the undulation has positive effects on the short term performance of the module. Similarly to Section 4.1.2.C, the curves obtained are not very clean, due to water droplets on the front side of the module and the constant change in light's incident angle in the solar module.

4.2 Mono-Si Experiments

In order to perform the experiments with another technology, two cells of Monocrystalline Silicon were used. The cells in question are from the Trina Solar TSM-DEG5-(II)-280 W panel and the technical Standard Testing Conditions specifications are in Table 4.2

Power [W]	4.6
Open Circuit Voltage [V]	4.25
Short Circuit Current [mA]	123

Table 4.2: Mono-Si cells specifications.

For the following experiments, two cells connected in series will be used, as shown in Figure 4.10:

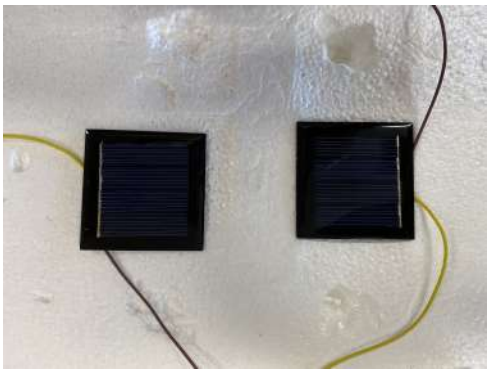

Figure 4.10: Mono-Si cells used to perform the experiments.

4.2.1 Establishing a base line for comparisons

Similarly to the previous technology, starting at room temperature, two I-V curves were obtained. The difference between them lies at the height of the lamp. The first experiment was performed at an height of 30 cm and the second one at the height of 15 cm.

The increase in radiation shows the increase in I_{SC}, which more than doubles when halving the height of the lamp. There is a small decrease in the value of V_{OC}, as would be expected due to the increase of the temperature of the module.

The resulting I-V curves of these experiments can be seen in Figure 4.11a and the corresponding P-V curves can be seen in Figure 4.11b.

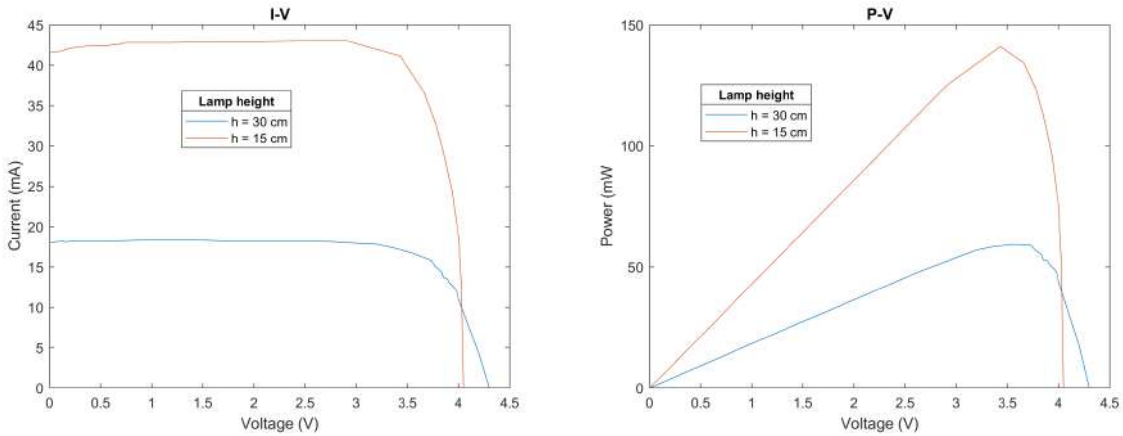

(a) I-V curves.

(b) P-V curves.

Figure 4.11: Mono-Si: baseline - experimental results.

By lowering the lamp, not only is the irradiance increasing, but also the temperature of the cells is increasing. In the second experiment, which took around 10 minutes to perform and the lamp was constantly turned on, there was an increase of 22℃ of the surface temperature of the module. Despite the short time it took to perform these experiments, the change in V_{OC} is significant.

The setup used to obtain the previous curves can be seen in Figure 4.12.

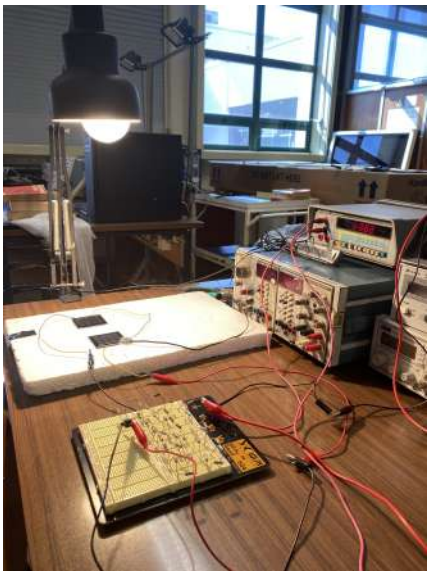

Figure 4.12: Experimental setup to obtain the baseline I-V curves of the Mono-Si cells.

At a first glance, one could say that Monocrystalline Silicon cells are more sensitive to the increase in radiation and temperature than CIGS modules, as was expected.

4.2.2 Floating experiments

Experiments were carried out to better understand the alterations that floating on water causes to the panels. In order to emulate a body of water, a plastic box containing tap water was used. While the CIGS modules could be in direct contact with water, Mono-Si modules do not present any water resistance. In order to conduct these experiments, the modules were put inside a clear plastic bag. This may cause some small changes to the final results due to the reflection and refraction of the light on the plastic above the cells. As in earlier floating studies, the modules were made to float using floats. In this situation, there was an attempt to prevent placing the floats directly beneath the solar cell and instead tried placing them on the cell's periphery, where there is simply plastic and no photoelectric material.

The influence of the water temperature will be analysed and the results will be presented. It will also be studied if there is any difference between stationary water for panels installed in lakes and dam reservoirs and waving water, for panels installed in sea.

4.2.2.A Fresh water at room temperature

The lamp in this experiment was placed at a distance of 15 cm from the solar module. The I-V and P-V curves were obtained, as well as the temperature of the module during the experiment. The water was

at room temperature, and at this point there was no attempt of either cooling or heating it.

The setup of this experience is shown in Figure 4.13.

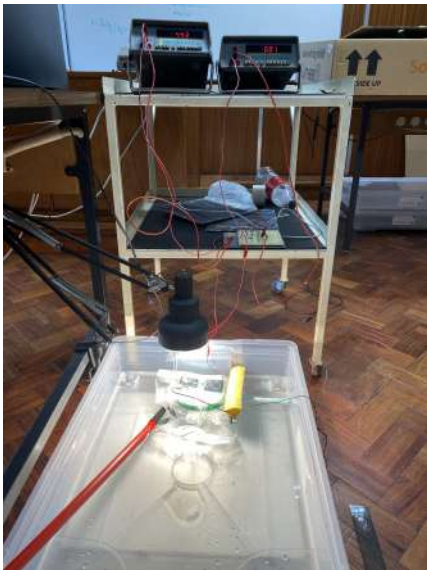

Figure 4.13: Experimental setup to obtain the I-V curve of the Mono-Si cells floating on water.

The red stick and the yellow sponge were utensils to help anchoring the cells, which were floating around, not allowing for an accurate reading of the values of the voltage and current.

In this experiment, it is expected that the I_{SC} will remain roughly the same, if not slightly higher than in the baseline, because of the light reflection on the water. The V_{OC} will not decrease since the module temperature will not increase as much compared to the previously established baseline.

The resulting I-V and P-V curves are presented in Figure 4.14:

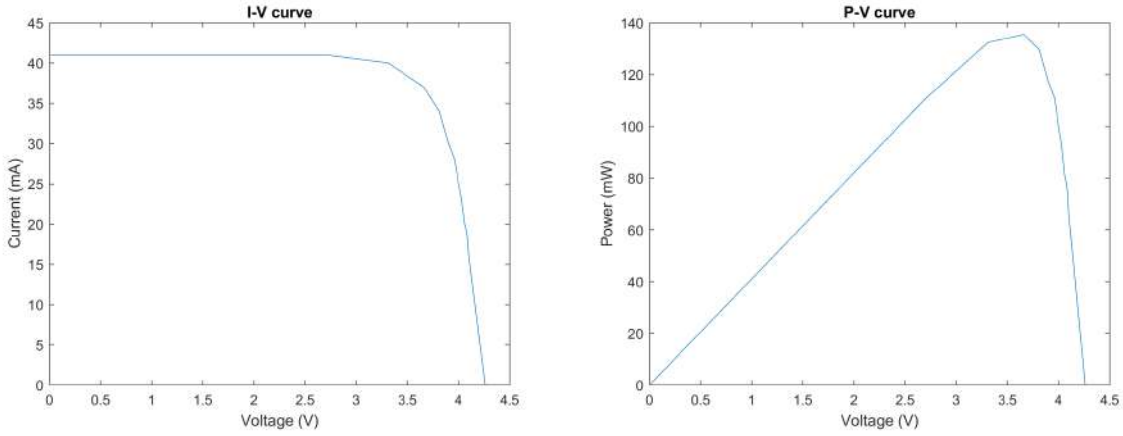

(a) I-V curve.

(b) P-V curve.

Figure 4.14: Mono-Si: floating in fresh water at room temperature - experimental results.

Comparing the findings of this experiment to those obtained for the same irradiance, that is, when the

lamp was positioned 15 cm above the solar module, the I_{SC} remained approximately the same, while the V_{OC} increased 0.2 V. Since both experiments took the same amount of time to perform, it can be inferred that floating modules are sightly more efficient, as one would anticipate.

The temperature of the cells rose 18 ℃ in the 10 minutes it took to perform the experiment, which is 4 ℃ less than that observed in the baseline.

4.2.2.B Fresh water cooled by ice

In order to analyse the effect that the water temperature has on floating systems, in the same setup as used previously, 4 kg of ice were added to the water. The I-V and P-V curves were obtained for the following water temperatures:

- **8.5 ℃**: the ice had been added a few minutes ago and it was still melting;
- **6 ℃**: the ice had just finished melting, the water was at its coldest temperature;
- **7 ℃**: the water was starting to increase its temperature.
- **12 ℃**: the water was increasing its temperature.

The setup used to perform this experiment is shown in Figure 4.15.

Figure 4.15: Experimental setup to obtain the I-V curves of the Mono-Si cells floating on water and ice.

It is expected that the colder the water, the higher the I_{SC}, as the temperature of the solar cells is not going to increase as to hinder the conversion efficiency. It is also expected that beyond a certain water temperature, the efficiency of the cells will be approximate to their efficiency with the water at room temperature, as the increase of the cells' temperature will be enough to impair the efficiency.

The results of the experiment are shown in the following Figure 4.16:

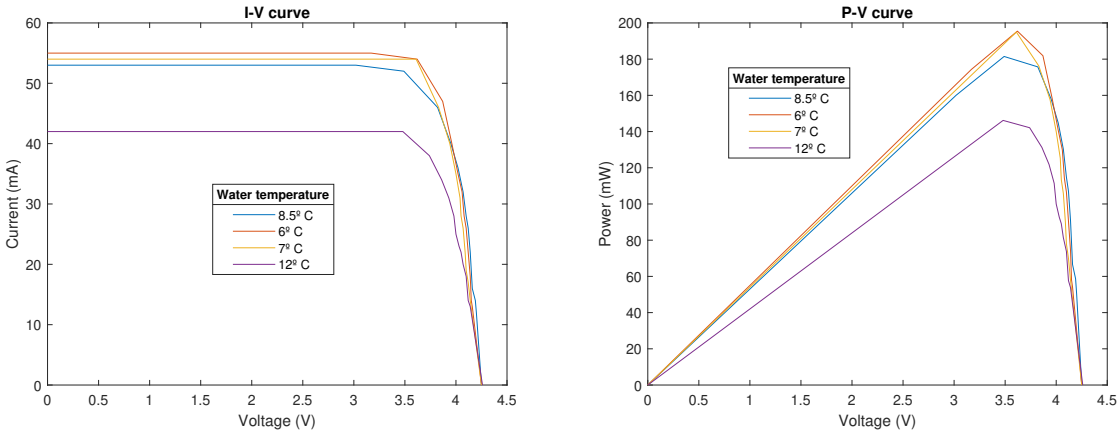

(a) I-V curve.

(b) P-V curve.

Figure 4.16: Mono-si: floating in fresh water cooled by ice - experimental results.

As can be seen in Figure 4.16, the colder the water, the higher the short circuit current as expected. There is no significant change in the value of the open circuit voltage.

There is a significant drop in the value of the current when the water temperature reaches 12 ℃ and the I_{SC} reaches the same value as it did in the experiment performed with water at room temperature.

The water temperature is the key in improving the efficiency of the floating panels. This could mean that this technology could prove to be very efficient in colder climate countries.

4.2.2.C Emulating waves in fresh water

Taking into account that under some very specific conditions floating parks can be installed in seas and not only lakes or reservoir dams, there was a need to study whether the movement of water had any effect on the performance of the solar modules.

The experimental setup is similar to the previous experiments: fresh water in a plastic box, the module set on floats at a distance of 15 cm from the lamp and the Mono-Si modules inside a clear plastic bag. In order to emulate waves, an electric mixer was used.

The results obtained in this experiment can be seen in Figure 4.17.

As seen with the CIGS modules, the curves obtained are not as smooth as the ones obtained for the other experiments, due to the movement of the water and the constant rocking of the modules, which affects the angle at which light reaches the module and, as a result, its absorption and energy conversion

In this experiment there was a 13 ℃ increase in the module's temperature. Similarly to what happened with the CIGS module, this result can be explained due to the ambient temperature being low on this day when compared to the previous experiments and due to the splashes of water that fall on the top of the module. Instead of the cooling being only done on the backside as in previous experiments, in this case cooling also happens on the front side, which prevents the temperature from rising as much.

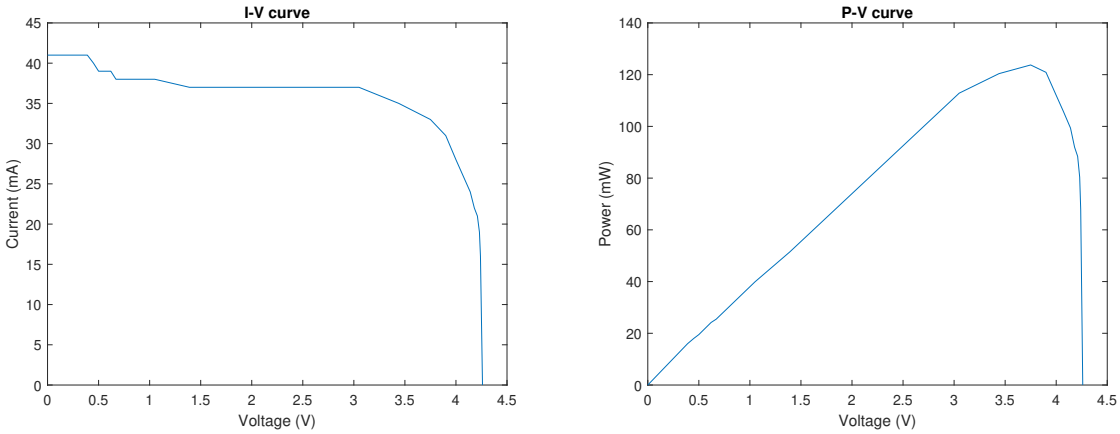

(a) I-V curves.

(b) P-V curves.

Figure 4.17: Mono-Si: emulating waves in fresh water - experimental results.

In the short run, this is a positive factor, however in the long run it It may have detrimental effects, as after the deposed water evaporates, foreign substances will be settled on the front of the panel, causing hotspots and in the longer run it may corrode and damage the front side of the panel altogether. This water deposition on the front side of the panel is more harmful in the case of silicon modules since they are not water resistant and are more susceptible to damages and corrosion. The negative effects can be avoided with frequent cleaning and maintenance of the panel, although it brings extra costs which may exceed the value of the extra energy produced.

4.2.2.D Emulating waves in fresh water cooled by ice

In order to evaluate the influence of the water temperature in the solar farms installed in the seas using Monocrystalline Silicon, an experiment was set up, where 4 kg of ice were added to the fresh water in the box as previously done and the waves were emulated with the electric mixer, as done in the last experiment.

The operating curves were obtained for the following water temperatures, which had been tested in Section 4.2.2.B:

- **6 ℃**: the ice had been melted for a while the water temperature was increasing;
- **7 ℃**: the water temperature was increasing, as well.

This was done to allow for a fair comparison between situations and extract reliable conclusions.

The I-V and P-V curves can be observed in Figure 4.18a and Figure 4.18b, respectively.

When the water was at 6 ℃, under these conditions, there was an increase in the module's temperature of 11.5 ℃, which is 1.5 ℃ less than in Section 4.2.2.B. There was no difference in the temperature of the module when the water was 7 ℃.

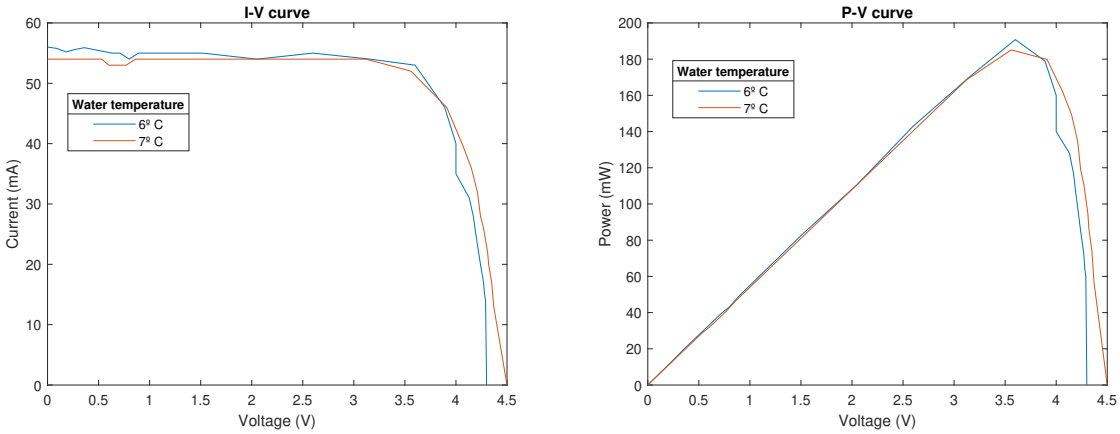

(a) I-V curves.

(b) P-V curves.

Figure 4.18: Mono-Si: emulating waves in fresh water cooled by ice - experimental results.

This smaller change in the module's temperature can be attributed to the silicon's higher temperature coefficient, when compared to that of the CIGS modules. Nevertheless, Mono-Si modules are still a safe bet and a good investment for floating solar farms. The smaller overall temperature increase allows for a higher I_{SC} and consequently a higher P_{max}.

As in previous situations in which undulation was emulated, the curves extracted are not as clean and stable when compared to curves obtained for simple floating situations. It is visible, however, the effects of the temperature in the I_{SC} and V_{OC}.

5

Simulations

Contents

5.1 CIGS technology simulations

To run simulations in *COMSOL Multiphysics* a 1D model of a CIGS cell was emulated. The base model is in COMSOL's database and it is for a sillicon model. With this being said, it needed adapting in order to be a CIGS model, which meant changing the base parameters of the material used, which are in Table 5.1.

Table 5.1: CIGS model properties

Property	Variable	Value	Unit
Relative permittivity	ϵ_r	13.6	-
Electron lifetime	τ_n	1.1×10^{-8}	s
Hole lifetime	τ_p	5×10^{-8}	s
Band gap	E_g	1.21	eV
Electron affinity	χ_e	4.21	eV
Effective density of states, valence band	N_c	1.6×10^{19}	cm^{-3}
Effective density of states, conduction band	N_v	2×10^{18}	cm^{-3}
Electron mobility	μ_n	100	$cm^2V^{-1}s^{-1}$
Hole mobility	μ_p	25	$cm^2V^{-1}s^{-1}$

Provided that this is a 1D approximation, some aspects must be taken into account in order to evaluate the results. A CIGS cell, as previously stated, is composed of several layers of different materials, which creates several *p p* junctions. These junctions generate electromagnetic fields, which in turn create disruptions in the electrons' mobility. This effect becomes visible in the I-V curve, and consequently P-V curve, obtained experimentally. However, the simulation does not consider these junctions, since it is a model which considers copper, indium, gallium and diselenide and the remaining composers of these types of cells to be a single material and not the layering of the several materials. This results in an altered I-V curve, with a straighter profile for the lower voltages as opposed to the real profile which presents itself with a tilted profile for the lower voltages.

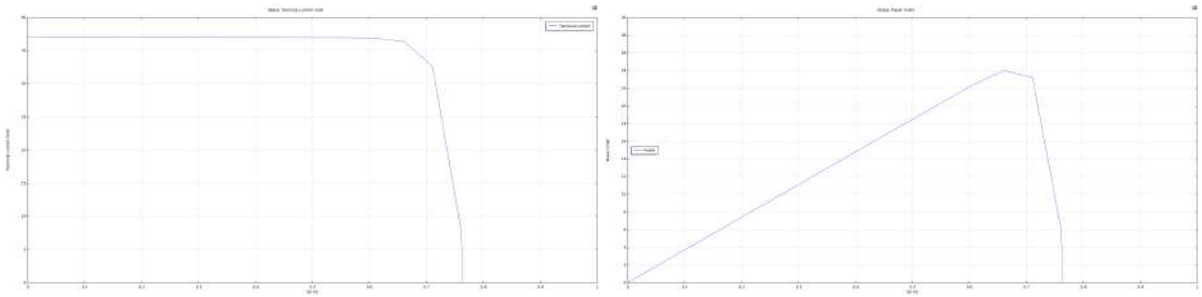

(a) I-V curve. **(b)** P-V curve.

Figure 5.1: CIGS curves obtained via simulation.

The values obtained from the I-V and P-V curves are summarised in Table 5.2.

Table 5.2: Values from the I-V and P-V curves.

I_{SC} [mA]	V_{OC} [V]	I_{mp} [mA]	V_{mp} [V]	P_{max} [mW]
18.7	0.76	36.3	0.66	24

5.2 Monocrystalline Silicon technology simulations

The base model that was adapted previously was now used to perform the simulation using a Monocrystalline Silicon cell. The model provided had the parameters shown in Table 5.3.

Table 5.3: Mono-Si model properties

Property	Variable	Value	Unit
Relative permittivity	ϵ_r	11.7	-
Electron lifetime	τ_n	10×10^{-6}	s
Hole lifetime	τ_p	10×10^{-6}	s
Band gap	E_g	1.12	eV
Electron affinity	χ_e	4.05	eV
Effective density of states, valence band	N_c	2.7×10^{19}	cm^{-3}
Effective density of states, conduction band	N_v	1.005×10^{19}	cm^{-3}
Electron mobility	μ_n	1450	$cm^2V^{-1}s^{-1}$
Hole mobility	μ_p	500	$cm^2V^{-1}s^{-1}$

This simulation presents curves very similar to the ones obtained experimentally. Since there are no electromagnetic fields due to *p p* junctions that disrupt the electrons' mobility as it happened in the CIGS simulation, we can conclude that this is a good approximation to what happens in reality. The theoretical and experimental curves are in conformity.

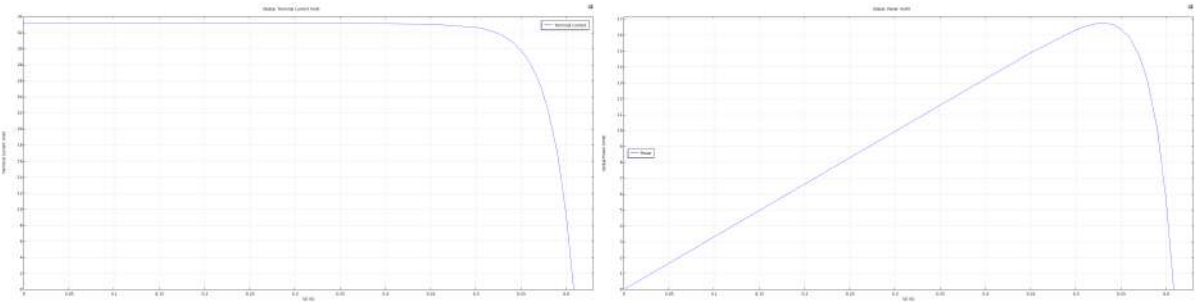

(a) I-V curve. **(b)** P-V curve.

Figure 5.2: Mono-Si curves obtained via simulation.

The values obtained from the I-V and P-V curves are summarised in Table 5.4.

Table 5.4: Values from the I-V and P-V curves.

I_{SC} [mA]	V_{OC} [V]	I_{mp} [mA]	V_{mp} [V]	P_{max} [mW]
33.15	0.61	31.63	0.53	16.76

6

Conclusions and Future Work

Contents

6.1 Conclusions

The literature review shows that decreasing the temperature of PV panels and consequently increasing their efficiency is possible. However, some methods do not yield enough energy after the cooling process to be deemed as effective. The cost analysis of some methods do prove them efficient and worthy of further investigation. The active cooling methods require more studies in order to evaluate if the extra energy produced compensates the energy used in the cooling process and if overall energy production increases.

The choice of studying floating systems deeper stems from the fact that these systems have been proved to be more efficient and are the most effective for bigger solar farms, whereas systems with either water or air circulation cannot be scaled for big parks and remain efficient. This is the most realistic approach for ”real life” systems and one that is predicted to continue being explored in years to come.

At first a baseline for both CIGS and Monocrystalline Silicon was created in order to establish comparisons with the following experiments and to allow for a conclusion to be drawn on whether or not there was an improvement with the experiments that were being performed. The temperature of the cells at the beginning and at the end of the experiment was registered. Later on, both solar modules were made to float on fresh water, which was at room temperature and their current-voltage curves were extracted. Both the water temperature and the cells temperature were registered. Comparing the temperatures of both solar modules, it was evident that the temperature had not risen as much as in the first experiment, and it was also noted that after a while the temperature stopped increasing at all, remaining stable for half of the time that it took to complete the measurements. The following experiment was set up in order to evaluate the influence that the water temperature has on solar modules. As was expected, the colder the water, the less the temperature increased, which meant higher short circuit current and, consequently, higher power and energy yield. With the Mono-Si modules it could also be seen that after a certain point, there was no influence of the water temperature, as the increase of the module temperature is very close whether the water had been cooled or not. Since under some conditions floating systems can be installed in oceans, there was also the need of studying whether the moving water had any extra effect on the temperature of the modules. When the water was at room temperature, it provided a considerable cooling effect, since there was water deposition on the front of the modules and running water on the back. The water on the front can pose some problems, as previously explained, but it helps with keeping the temperature down. Afterwards, the influence of the moving colder water was investigated, and as anticipated, the colder water proved to be more efficient at keeping the modules colder and providing more power. Nevertheless, they present the same problem with the deposition of water on the front. It can be tackled with a cleaning team that goes to the location occasionally. This will, however, bring extra costs.

It can be concluded that floating systems are, overall, an improvement to the typically ground-mounted systems. They are a good investment, particularly in colder climate countries, as the water will be at a lower temperature, allowing for a smaller and less affecting temperature rise of the modules.

Tables summarising the experiments and their findings are shown next (see Table 6.1 for results of the CIGS modules and Table 6.2 for results of Mono-Si modules).

Table 6.1: Summary of temperature increases for CIGS technology.

Situation	Water Temperature [°C]	Temperature Increase [°C]
Baseline	-	10
Floating in fresh water	20	5
Floating in fresh water cooled by ice	8 5.5 6 7	3.5 1.5 2.5 3
Emulating waves in fresh water	13	1.5
Emulating waves in fresh water cooled by ice	1.2 5.5	0.5 1

Table 6.2: Summary of temperature increases for Mono-Si technology.

Situation	Water Temperature [°C]	Temperature Increase [°C]
Baseline	-	22
Floating in fresh water	20	18
Floating in fresh water cooled by ice	8.5 6 7 12	14 13 13.5 17
Emulating waves in fresh water	13	13
Emulating waves in fresh water cooled by ice	6 7	11.5 13.5

The simulations performed using *COMSOL Multiphysics* allowed for the establishment of the I-V and P-V curves that were expected to be obtained during the practical experiments. However, the CIGS curve simulated was not similar to the one obtained through experiment, given the 1D approximation and the non-existence of the *p p* junctions that are present in the real modules.

6.2 Future Work

The simulations were carried out using a 1D model, which lacks the depth needed to properly evaluate a CIGS module. In a future work 2D and/or 3D models should be developed in order to provide more reliable simulation results.

Mathematical models should also be developed in order to be able to optimise future systems. They could work by taking into account the average temperature of the waters, according to the season, and

predict the short circuit current increase and consequent power increase. This could be used on a later stance to predict the amount of energy which will be produced by solar farms and allow the market to react accordingly.

In future works regarding the experimental results, instead of using a lamp in the laboratory to produce results, carrying out some of the experiments outside using sun light might provide more accurate results and result in an even better understanding of the cooling effect that happens to floating systems.

The consequences of floating systems in the existing ecosystems of the dams, lakes, and seas where they are installed must be studied, namely, the impact in the oxygen levels of the water, the life cycle of animals and whether there is pollution originated by the floating systems.

Bibliography

[1] R. Castro, “Slides from curricular unit: Energias renováveis e produção descentralizada,” 2002.

[2] M. Hasanuzzaman, A. B. M. A. Malek, M. M. Islam, A. K. Pandey, N. A. Rahim, “Global advancement of cooling technologies for pv systems: A review,” *Solar Energy*, no. 137, pp. 25–45, 2016.

[3] J. Siecker, K. Kusakana, B. P. Numbi, “A review of solar photovoltaic systems cooling technologies,” *Renewable and Sustainable Energy Reviews*, vol. 79, pp. 192–203, May 2017.

[4] Mohamed R. Gomaa, Mujahed Al-Dhaifallah, Ali Alahmer, Hegazy Rezk, “Design, modeling, and experimental investigation of active water cooling concentrating photovoltaic system,” *MDPI, Sustainability*, no. 12, 2020.

[5] Z. Farhana, Y.M. Irwan, R.M.N. Azimmi, A.R.N. Razliana, N. Gomesh, “Experimental investigation of photovoltaic modules cooling system,” pp. 165–169, 2012.

[6] Jan Wajs, Aleksandra Golabek, Roksana Bochniak, “Photovoltaic roof tiles: The influence of heat recovery on overall performance,” *MDPI, Energies*, October 2019.

[7] Oussama Rejeb, Mohammad Sardarabadi, Christophe Ménézo, Mohammad Passandideh-Fard, Mohamed Houcine Dhaou, Abdelmajid Jemni, “Numerical and model validation of uncovered nanofluid sheet and tube type photovoltaic thermal solar system,” *Energy Conversion Management*, vol. 110, pp. 367–377, November 2015.

[8] Preeti Singh, Sourav Khanna,Sanjeev Newar, Vashi Sharma, K. Srinivas Reddy, Tapas K. Mallick, Victor Becerra, Jovana Radulovic, David Hutchinson, Rinat Khusainov, “Solar photovoltaic panels with finned phase change material heat sinks,” *MDPI, Energies*, vol. 13, May 2020.

[9] Lin J. Simpson, Jason Woods, Nicolas Valderrama, Alex Hill, Nina Vincent, Timothy Silverman, “Passive cooling of photovoltaics with desiccants,” *IEEE*, 2017.

[10] Belkacem Zouak, Aghiles Ardjal, Maamar Bettayeb, Rachid Zirmi, Mohammed Said Belkaid, “System of cooling and improving power output of photovoltaic solar cells,” *Advances in Science and Engineering Technology International Conferences*, 2020.

[11] Slawomir Gulkowski, Agata Zdyb, Piotr Dragan , "Experimental efficiency analysis of a photovoltaic system with different module technologies under temperate climate conditions," *Applied Sciences*, no. 141, January 2019.

[12] U. Nations, "The 17 goals = Available at https://sdgs.un.org/goals (2021/05/15)."

[13] A. Jäger-Waldau, "Pv status report 2019," JRC Science for Policy Report, Report P-50, 2019.

[14] F. Shan, F. Tang, L. Cao, G. Fang, "Comparative simulation analyses on dynamic performances of photovoltaic–thermal solar collectors with different configurations," *Energy Conversion Management*, vol. 87, pp. 778–786, August 2014.

[15] M. M Rahman, M. M. Hasanuzzaman, N. A. Rahim, "Effects of various parameters on pv-module power and efficiency," *Energy Conversion Management*, vol. 103, pp. 3348–33 558, July 2015.

[16] Himanshu Sainthiya, Narendra S. Beniwal, "Different types of cooling systems used in photovoltaic module solar system: A review," *IEEE*, pp. 1500–1506, 2017.

[17] Pearlyn J.Y. Chua, Stephen E. R. Tay, "Comparative discussion of active and passive cooling of pv modules - are we doing it right?" 2020.

[18] Haitham M. Bahaidarah, Shafiqur Rehman, P. Gandhidasan, and Bilal Tanweer, "Experimental evaluation of the performance of a photovoltaic panel with water cooling," 2013.

[19] Vinicius Silva, Julio Martinez, Raphael Heideier, Jonathas Bernal, Andre Gimenes, Miguel Udaeta, Marco Saidel, "A long-term analysis of the architecture and operation of water film cooling system for commercial pv modules," *MDPI, Energies*, no. 14, March 2021.

[20] Amit Sahaya, V. K. Sethib, A. C. Tiwaric, Mukesh Pandey, "A review of solar photovoltaic panel cooling systems with special reference to ground coupled central panel cooling system (gc-cpcs)," *Renewable and Sustainable Energy Reviews*, vol. 42, pp. 306–312, February 2015.

[21] M. Elmira, R. Mehdaouia, A. Mojtabib, "Numerical simulation of cooling a solar cell by forced convection in the presence of a nanofluid," *Energy Procedia*, vol. 18, no. 8, pp. 594–603, 2012.

[22] M. Imtiaz Hussain, Jin-Hee Kim, Jun-Tae Kim, "Nanofluid-powered dual-fluid photovoltaic/thermal (pv/t) system: Comparative numerical study," *MDPI, Energies*, no. 12, February 2019.

[23] W. Mackenzie, "Floating solar landscape 2019 = Available at https://www.woodmac.com/our-expertise/focus/Power--Renewables/floating-solar-2019/?utm_source=gtmarticle&utm_medium=web&utm_campaign=wmpr_floatingsolar (2019/09/19)."

[24] A.A. Jadallaha, D.Y. Mahmooda, Z. Erb, Z.A. Abdulqaedr, “Hybridization of solar/wind energy system for power generation in rural areas,” *2nd International Conference on Computational and Experimental Science and Engineering*, vol. 130, pp. 434–437, 2016.

[25] I. F. C. W. B. Group, “Floating solar photovoltaic on the rise = Available at https://www.ifc.org/wps/wcm/connect/6ef92aa8-bf29-4c43-8edc-a0f7555e6a5d/IFC-EnergyNotes-FloatingSolar_WEB.pdf?MOD=AJPERES&CVID=n8KDCtS (2020/05) .”

[26] Pietro Elia Campana, Louise Wästhagea, Worrada Nookueaa, Yuting Tanb, Jinyue Yan, “Optimization and assessment of floating and floating-tracking pv systems integrated in on- and off-grid hybrid energy systems,” *Solar Energy*, no. 117, pp. 782–795, 2019.

[27] Alok Sahu, Neha Yadav, K. Sudhakar, “Floating photovoltaic power plant: A review,” *Renewable and Sustainable Energy Reviews*, vol. 66, pp. 815–824, 2016.

[28] EDP, “Floating solar panels = Available at https://www.edp.com/en/innovation/floating-solar-pannels .”

[29] ——, “Construção do parque solar flutuante da edp no alqueva vai arrancar = Available at https://www.edp.com/pt-pt/noticias/2021/05/11/construcao-do-parque-solar-flutuante-da-edp-no-alqueva-vai-arrancar .”

[30] Reuters, “Singapore unveils one of the world’s biggest floating solar panel farms = Available at https://www.reuters.com/business/energy/singapore-unveils-one-worlds-biggest-floating-solar-panel-farms-2021-07-14/ (2021/07/14) .”

[31] S. D. Sharma, H. Kitano, K. Sagara, “Phase change materials for low temperature solar thermal applications,” *Energy*, vol. 29, pp. 31–64, September 2004.

[32] W.G.J.H.M. van Sark, “Feasibility of photovoltaic – thermoelectric hybrid modules,” *Applied Energy*, vol. 88, no. 8, pp. 2785–2790, March 2011.

[33] José Antonio Luceño-Sánchez, Ana María Díez-Pascual, Rafael Peña Capilla, “Materials for photovoltaics: State of art and recent developments,” *International Journal of Molecular Sciences*, vol. 20, no. 976, February 2019.

[34] Shigeru Niki, Miguel Contreras, Ingrid Repins, Michael Powalla, Katsumi Kushiya, Shogo Ishizuka, Koji Matsubara, “Cigs absorbers and processes,” *Progress in Photovoltaics: Research and Applications*, vol. 18, no. 6, pp. 453–466, August 2010.

[35] Thomas Feurer, Patrick Reinhard, Enrico Avancini, Benjamin Bissig, Johannes Löckinger, Peter Fuchs, Romain Carron, Thomas Paul Weiss, Julian Perrenoud, Stephan Stutterheim, Stephan Buecheler, Ayodhya N. Tiwari, "Progress in thin film cigs photovoltaics – research and development, manufacturing, and applications," *Progress in Photovoltaics: Research and Applications*, vol. 25, no. 7, pp. 645–667, October 2016.

[36] K. D. G. Imalka Jayawardena, Lynn J. Rozanski, Chris A. Mills, Michail J. Beliatis, N. Aamina Nismya, S. Ravi P. Silva, "'inorganics-in-organics': recent developments and outlook for 4g polymer solar cells," *Nanoscale*, vol. 5, pp. 8411–8427, July 2013.

[37] Daniela Dirnberger, Gina Blackburn, Björn Müller, Christian Reise, "On the impact of solar spectral irradiance on the yield of different pv technologies," *Solar Energy Materials and Solar Cells*, vol. 132, pp. 431–442, January 2015.

[38] Claudia Brusdeylins, "Press release: New best mark in thin-film solar performance with 21.7 percent efficiency," September 2014.

[39] B. P. Jelle, C. Breivik, "The path to the building integrated photovoltaics of tomorrow," *Energy Procedia*, vol. 20, pp. 78–87, 2012.

[40] Samar Dabbabi, Tarek Ben Nasr, Najoua Turki Kamoun , "Cigs solar cells for space applications: Numerical simulation of the effect of traps created by high-energy electron and proton irradiation on the performance of solar cells," *The Journal of The Minerals, Metals & Materials Society (TMS)*, no. 71, p. 602–607, February 2018.

[41] I. Ascent Solar Technologies, "Nasa's marshall space flight center selects ascent solar technologies cigs modules for their lisa-t and solar cruiser flight experiments = Available at https://www.globenewswire.com/en/news-release/2021/03/01/2184008/0/en/NASA-s-Marshall-Space-Flight-Center-Selects-Ascent-Solar-Technologies-CIGS-Modules-for-Their-LISA-T-and-S html ."

[42] L.A. Dobrzański, A. Drygała, M. Giedroć, M. Macek, "Monocrystalline silicon solar cells applied in photovoltaic system," *Journal of Achievements in Materials and Manufacturing Engineering*, vol. 53, no. 1, pp. 7–13, July 2012.

[43] *Uma Introdução Às Energias Renováveis: Eólica, Fotovoltaica e Mini-hidríca*. IST Press, 2011.

[44] S. B. Hub, "Monocrystalline silicon wafers market share expected to reach nearly 75 percent in 2020 and continue to grow, itrpv report finds = Available at https://solarbusinesshub.com/2020/05/08/monocrystalline-silicon-wafers-market-share-expected-to-reach-nearly-75-percent-in-2020-and-continue-to-grow ."

[45] D. B. M. Research, “Global monocrystalline solar cell (mono-si) market – industry trends and forecast to 2027 = Available at https://www.databridgemarketresearch.com/reports/global-monocrystalline-solar-cell-mono-si-market .”